IET Nanobiotechnology

Research Article

IET Journals
The Institution of Engineering and Technology

Modification of rheological and filtration characteristics of water-based mud for drilling oil and gas wells using green SiO_2@ZnO@Xanthan nanocomposite

ISSN 1751-8741
Received on 13th July 2018
Revised 28th May 2019
Accepted on 14th June 2019
E-First on 29th July 2019
doi: 10.1049/iet-nbt.2018.5205
www.ietdl.org

Jagar A. Ali[1,2] ✉, Kamal Kolo[3], S. Mohammad Sajadi[4,5], Karmand H. Hamad[1], Rida Salman[1], Mariam Wanli[1], Abbas Khaksar Manshad[1,6], Samir M. Hamad[3], Buya Raihana[1], Sarkar Muheedin Hama[1]

[1]*Department of Petroleum Engineering, Faculty of Engineering, Soran University, Soran, Kurdistan Region, Iraq*
[2]*Department of Petroleum Engineering, College of Engineering, Knowledge University, Erbil, Kurdistan Region, Iraq*
[3]*Scientific Research Centre, Soran University, Soran, Kurdistan Region, Iraq*
[4]*Department of Petroleum Geoscience, Faculty of Science, Soran University, PO Box 624, Soran, Kurdistan Regional Government, Iraq*
[5]*Department of Nutrition, Cihan University-Erbil, Kurdistan Region, Iraq*
[6]*Department of Petroleum Engineering, Abadan Faculty of Petroleum Engineering, Petroleum University of Technology (PUT), Abadan, Iran*
✉ *E-mail: jagar.ali20@gmail.com*

Abstract: In this study, a green, simple and economical approach was used to synthesise the SiO_2@ZnO@Xanthan nanocomposite (NC) to modify the rheological and filtration characteristics of the water-based drilling mud. The green synthesised NCs were identified using scanning electron microscopy, energy dispersive X-ray spectroscopy, elemental mapping, X-ray diffraction and UV–Vis analytical techniques. Additionally, the effect of SiO_2@ZnO@Xanthan NCs on the filtration and rheological properties of mud including apparent viscosity, plastic viscosity, yield point, gel strength, mud cake and fluid loss was investigated. The obtained results confirmed that the synthesised NCs effectively improved the rheological properties of drilling mud, and considerably decreased its fluid loss and filter cake by about 54 and 92.5%, respectively. The results highly recommend the SiO_2@ZnO@Xanthan NC as an excellent additive to improve the rheological properties, and reduce the fluid loss and the filter cake of the drilling mud.

1 Introduction

As non-Newtonian fluids, the viscosity of drilling mud decreases on increasing the shear rates [1, 2]. To suspend the drilled rock cuttings during drilling and carrying them out of the borehole to the surface efficiently, it is essential to have a drilling mud with high viscosity and low shear rates. However, to circulate the drilling fluid down into the borehole with a better flow and low resistance, drilling fluids must have low viscosity at high shear rates. For these reasons, numerous chemical additives have been used to improve the rheological performance of drilling fluids [2, 3, 4]. Nowadays, researchers are trying to use nanoparticles (NPs) due to their excellent rheological properties and environmental benefits for providing a drilling fluid with better performance in borehole cleaning and cutting process [5–10]. Furthermore, an ideal drilling mud needs to have preferred filtration properties, such as an acceptable range of fluid loss into the formation and practical thickness of the mud cake on the wall of the wellbore. Thereby, some of the borehole problems can be eliminated, for example, the differential sticking, lost circulation and wellbore collapse [11].

The metal and metal oxide NPs are of great importance due to their large applications in industry and medicine. In fact, these applications benefit from their large surface area and number of active sites per unit area compared to the parent metal. Previous methods of NP synthesis suffer from the harsh synthesis conditions and high costs, but nowadays, the greener and more ecofriendly ways, especially the use of plants removes all these challenges and also increases the stability of produced nanostructures by altering their sensitivity to oxygen, water and other chemical entities [12, 13]. Agglomeration of NPs due to their surface potential is an interest of researchers of the field to prevent this problem and the overstoichiometric use of metal reagents, application of bio-supports for the deposition of metal NPs which provides both a cost-effective and green way for the nanocomposite (NC) production is the current policy of the researchers. Ranjbar *et al.* [14, 15] enabled the synthesis of ZnO nanorod coated by SiO_2 and SiO_2–TiO_2 NCs using the hydrothermal method. Xanthan gum is a complex exopolysaccharide, produced by plant-pathogenic bacterium. Xanthan gum is widely used as a thickening and stabilising agent in a wide variety of food and industrial products. During this study, we employed this bio-support for the deposition of green-synthesised SiO_2 NPs and ZnO NPs and finally the fabrication of SiO_2@ZnO@Xanthan NC. Researchers are interested in the screening and identification of new antioxidants from the plant sources. Antioxidant activity in plant extract is due to the redox potential of phytochemicals to quench the singlet and triplet oxygen, decomposing the peroxides or neutralising the free radicals. Higher bioactivity of NPs is due to the large surface of NPs and preferential adsorption of the bioactive material such as the bioactive phytochemicals from the extract onto the surface of the NPs which are strongly affected by the surface area, particle size and surface reactivity of the NPs [16–19].

Pomegranate is an important source of bioactive compounds with potent antioxidant activity (Fig. 1). Numerous studies reported the presence of considerable antioxidants and bioactive phytochemicals such as phenolics, flavonoids, anthocyanidins and ascorbic acids inside the seed fractions of pomegranate [20, 21]. In continuation of our previous researches on the green synthesis of NPs, in this study [22–25], the SiO_2@ZnO@Xanthan NCs was green-synthesised using pomegranate seed extract as an efficient nano-adsorbent substrate for the filtration of water-based drilling mud.

Fig. 1 *Pomegranate and its seeds*

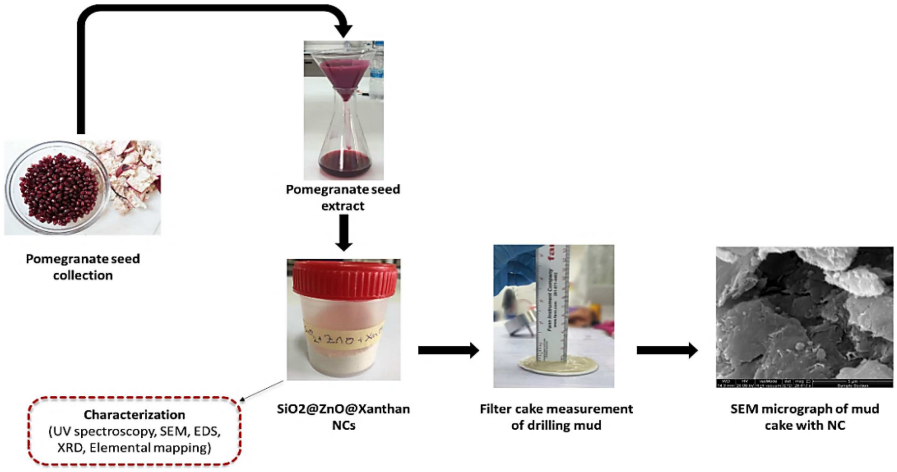

Fig. 2 *Schematic diagram shows the typical procedure for the synthesis of NCs and their application in drilling fluid*

Table 1 Formulation of NC drilling fluid

Sample	Drilling mud (nanofluid)
S1	WB
S2	WB + 0.02 wt.% NC
S3	WB + 0.05 wt.% NC
S4	WB + 0.10 wt.% NC
S5	WB + 0.20 wt.% NC
S6	WB + 0.50 wt.% NC

2 Materials and methodology

2.1 Instruments and reagents

High-purity chemical reagents including salts and solvents were purchased from the Merck and Aldrich chemical companies. Xanthan gum and bentonite were used in standard quality. All analyses were performed at Soran University Scientific Research Centre. X-ray diffraction (XRD) measurements were carried out using a Philips powder diffractometer type PW 1373 goniometer (Cu Kα = 1.5406 Å). The scanning rate was 2°/min in the 2θ range from 10 to 90°. Scanning electron microscopy (SEM) was performed on a Cam scan MV2300. EDS (S3700N) was utilised for the chemical analysis of prepared nanostructures. The UV–visible measurements were performed at room temperature by a Perkin Elmer 550ES from 200 to 600 nm at a resolution of 1 nm.

2.2 On-pot biosynthesis of SiO_2@ZnO@Xanthan NCs

In a 500 ml flask, 2 g sodium meta silicate, 5 g $ZnCl_2$ and 10 g Xanthan powder were mixed in 200 ml pomegranate seed extract under reflux condition at 80°C while stirring for 2 h until the formation of a light black precipitate. The precipitate then was separated using filtration and washed with hot distillate water many times to remove impurities. The clean precipitate then was dried at room temperature for further use (Fig. 2).

2.3 Preparation of the drilling fluid samples

The drilling mud was prepared based on the API standard specifications by adding 20 g of bentonite, 0.5 g of sodium hydroxide, 0.5 g of soda ash and 0.5–5 g of starch stirred at 11,000 rpm by a commercial Hamilton Beach stirrer. Afterwards, five different samples of nanofluids were prepared by adding the green NC into water-based mud (WB) at a concentration ranging from 0.02 to 0.5 wt.% (see Table 1).

2.4 Rheological measurements of drilling mud

The rheological properties of all samples (see Table 1) including apparent viscosity, plastic viscosity, yield point and gel strength of the drilling fluids were measured using the FANN 35 viscometer (Scheme 1) from which the rheological parameters were calculated

$$\mu_p = 600\,\text{rpm reading} - 300\,\text{rpm reading} \quad (1)$$

$$\mu_a = 600\,\text{rpm reading}/2 \quad (2)$$

$$\tau_y = 300\,\text{rpm reading} - \mu_p \quad (3)$$

where μ_p is plastic viscosity in cP, μ_a is apparent viscosity in cP and τ_y is yield point in Ib/100 ft^2.

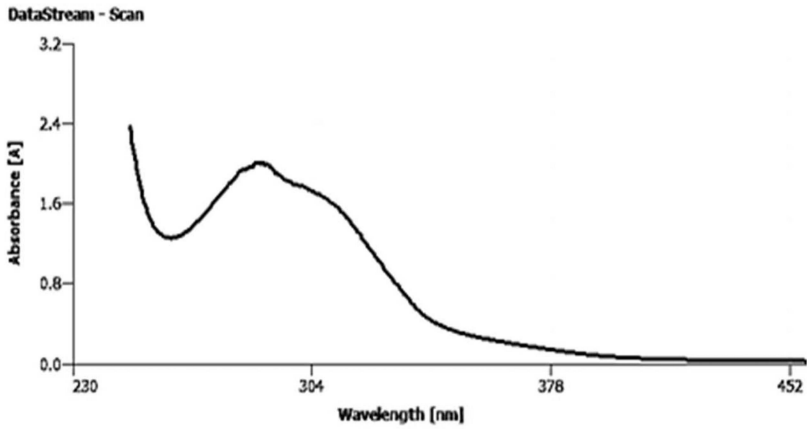

Fig. 3 *UV-vis spectroscopy of pomegranate seed extract used in the synthesis of SiO_2@ZnO@Xanthan NCs*

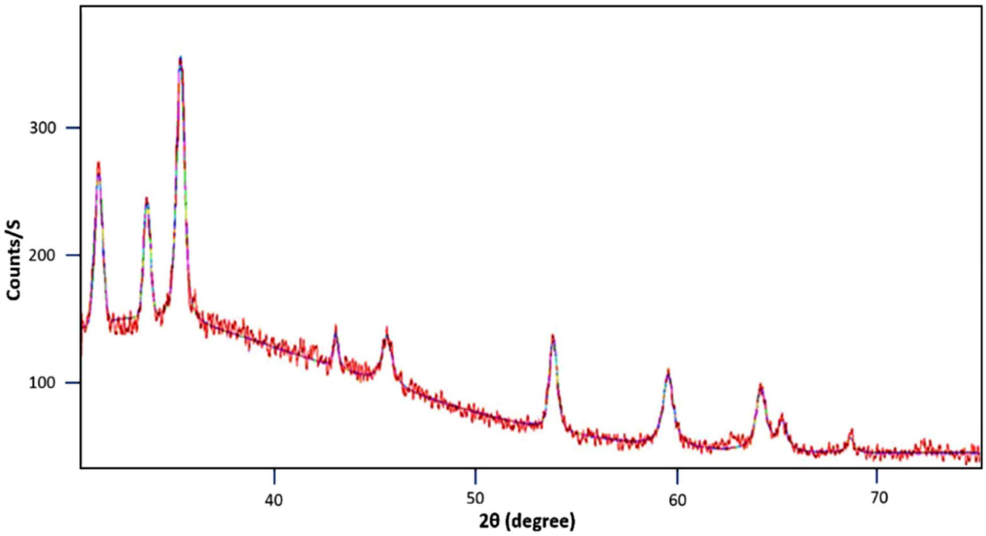

Fig. 4 *XRD pattern of the SiO_2@ZnO@Xanthan NCs*

Shear stresses and shear rates were also determined from the measured deflections of various speeds of the rotational viscometer. Following the API standard procedure, the gel strength of the drilling fluids was measured at 10 s and 10 min setting times.

2.5 Filtration measurements of drilling mud

The filtration properties including both filter cake and fluid loss were studied using a Series 300 LPLT Filter Press at 100 psi and room temperature. The filter cake thickness was measured after 30 min and the fluid loss measurements were taken at time intervals between 0 and 30 min (see Table 1).

3 Results and discussion

3.1 Identification of the plant extract

The UV–Vis spectroscopy of the pomegranate extract shows specified bands of phenolics at 312 nm (band I) and 285 nm (band II) due to the transition localised within the ring of cinnamoyl and benzoyl systems, respectively (Fig. 3). This spectrum strongly confirmed the presence of potent antioxidants inside the plant extract and therefore supports the results obtained by previous reported literature about the plant.

3.2 Identification of green synthesised NCs

Fig. 4 shows a typical XRD pattern of SiO_2@ZnO@Xanthan NCs which contains all the peaks associated with the crystalline planes of pure SiO_2 and ZnO NPs concerning the crystallinity and phase purity of NPs deposited on the surface of xanthan. No other diffraction peaks indicating the impurities present in the XRD pattern indicate the high phase purity of synthesised NCs. Moreover, based on the XRD patterns of SiO_2@ZnO@Xanthan NCs with respect to the *Sherrer's* equation (4), the average crystallite size of the SiO_2 and ZnO NPs deposited on the substrate is found to be 25 and 80 nm respectively

$$D = \frac{K\lambda}{\beta\cos\theta} \tag{4}$$

where D is crystallite size, λ is wavelength in nm, K is shape factor between 0.62 and 2.08 (0.89 was taken), β is the width of peak in 2θ and θ is the Bragg angle.

Fig. 5 shows SEM micrographs of the synthesised NCs. It clearly indicated that the SiO_2 and ZnO NPs deposited well on the xanthan substrate surface. Also based on the SEM image, the NPs are uniformly distributed on the surface of the xanthan substrate. For further confirmation concerning the biosynthesis of NCs, energy dispersive X-ray spectroscopy (EDX) and elemental mapping were applied. EDX and elemental mapping strongly depicted the presence of Si, Zn, O, Na and Ca elements as the elemental composition of NCs. Both techniques again strongly show the fabrication of NCs using the green method (Figs. 6 and 7).

3.3 Rheological properties

It was identified that the suspension of NCs within the water-based mud has a shear thinning behaviour with low viscosity at high shear rates and high viscosity at low shear rates. This behaviour increases on increasing the concentration of NCs. In this study, we

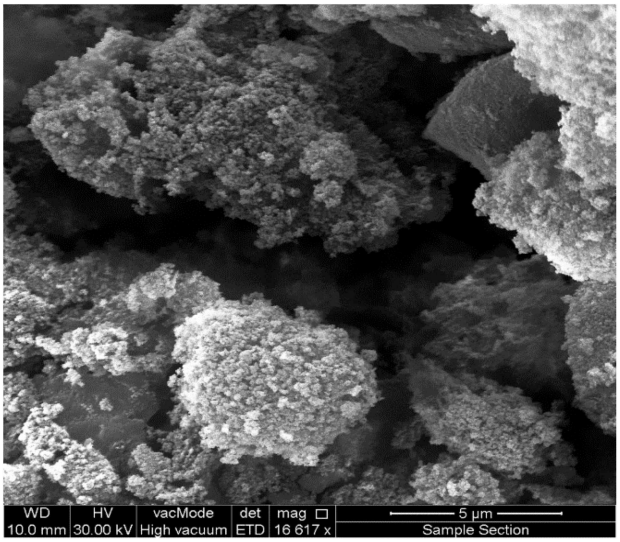

Fig. 5 *SEM micrograph of SiO_2@ZnO@Xanthan NCs showing NPs morphology, size and their adherence to the Xanthan substrate particles*

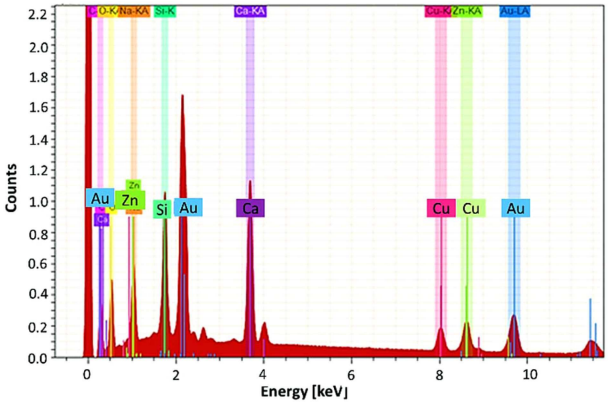

Fig. 6 *EDX spectrum of the green synthesised NCs obtained from area EDX analysis on a selected NCs grain showing the elemental composition of Zn, Si, Ca and Cu. Au is from sputtering gold coating*

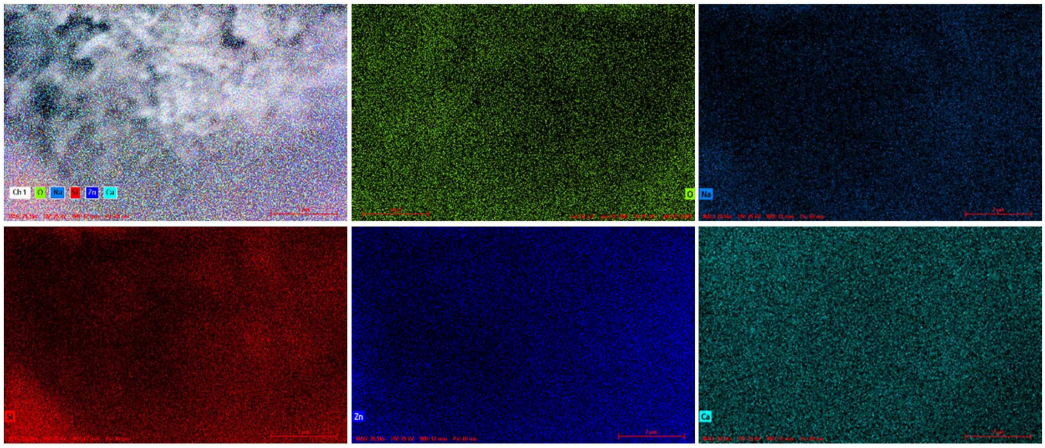

Fig. 7 *EDX elemental mapping analysis of green synthesised NCs*

added NCs with different concentrations (0.02–0.5 wt.%) into the base drilling mud (WB). The effect of NCs and their concentration on the rheological properties of the drilling fluid is shown in Table 2.

From the results, it can be seen that the values of all the rheological properties of drilling mud include plastic viscosity, apparent viscosity, yield point and gel strengths were increased after adding NCs into the mud. Although considerable changes in the rheological properties of mud occurred, the percentage of increase in the gel strength property of the mud was higher with about 100–150%, compared to the base mud. The base drilling mud showed a very poor shear thinning behaviour, which has the lowest values of plastic viscosity and apparent viscosity was found to be about 9 and 23.5 cP, respectively. While after adding the NCs into the WB mud at different concentrations, various drilling muds with better shear thinning behaviour were obtained as shown in Fig. 8. The viscosity of the drilling mud increased when the concentration of NCs in the mud increased. In S2, by adding only 0.08 g of NCs into the WB, the plastic viscosity and apparent viscosity of the fluid were increased from 9 and 23.5 cP to 10 and 25 cP, respectively (see Table 2). Additionally, a modification in the thinning behaviour of the mud occurred, in which higher viscosity was achieved at the same shear rate. The shear rates were determined from different deflections of the viscometer at 3, 6,

Table 2 Rheological properties of the drilling fluids without and with NCs at different concentrations

Mud sample	μ_α, cp	μ_P, cp	τ_y, lb/100 ft^2	Gel strength, lb/100 ft^2	
				$Gel_{initial}$	Gel_{final}
S1 (WB)	23.5	9	25	13	20
S2 (WB + 0.02 wt.% NC)	25	10	30	16	22
S3 (WB + 0.05 wt.% NC)	28	12	32	19	23
S4 (WB + 0.10 wt.% NC)	34	17	34	21	26
S5 (WB + 0.20 wt.% NC)	39	21	36	29	35
S6 (WB + 0.50 wt.% NC)	40	22	37	41	49

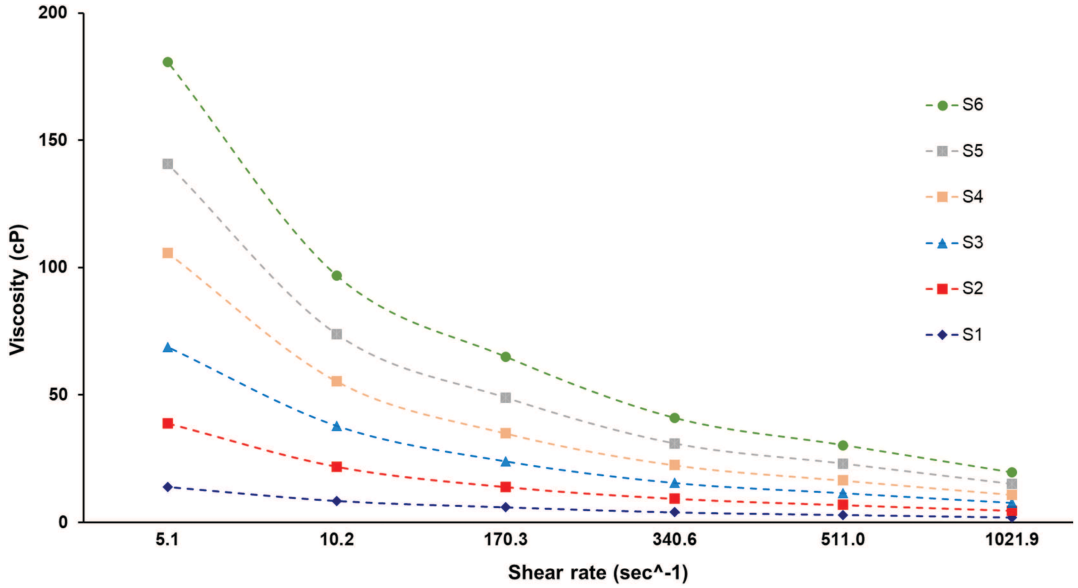

Fig. 8 *Viscosity as functions of shear rates for the fluids with different concentrations SiO_2@ZnO@Xanthan NCs estimated from the deflection of 3, 6, 100, 200, 300 and 600 rpm of the rotational viscometer*

100, 200, 300 and 600 rpm. From increasing the concentration of NCs, the rheological properties including the viscosity, yield point and gel strength of the drilling fluids continued to rise (see Table 2). As it can be seen, the apparent viscosity and plastic viscosity of S6, which contains the highest amount of NCs, increased by 70 and 144%, compared to S2 mud with the lowest concentration of NCs, from 23.5 and 9 cP to 40 and 22 cP, respectively. In this case, it was identified that the performance of the drilling fluids can be maintained and possibly improved by adding a small percentage of the NCs. Accordingly, the solid content of the drilling fluids would be reduced because of using small amounts of additives. As a result, a faster drilling rate, better and easier solid control, easier re-functioning of the mud, improved hydraulic and less formation damage can be achieved.

The yield stresses of the drilling fluids were gradually increased by adding the NCs. The yield stress of S1 drilling mud was calculated to be about 25 lb/100 ft^2 and it increased to 30 lb/100 ft^2 by adding only 0.08 g of NC. While the value of this property was increased significantly to 37 lb/100 ft^2 when the concentration of the NC inside the drilling mud increased by about 0.5 wt.%. In terms of gel strength of the drilling mud, both initial and final values of gel strength were improved by increasing the amount of NCs in the drilling fluids. As the lowest loading level (0.08 g) of NCs was added, the measured values of gel strength at 10 s and 10 min were equal to 16 lb/100 ft^2 and 22 lb/100 ft^2, respectively. However, the values of gel strength at 10 s and gel strength at 10 min were greatly increased to 41 lb/100 ft^2 and 49 lb/100 ft^2 after increasing the concentration of NCs by 0.5 wt.%. This improvement in yield point and gel strength properties was observed (Fig. 9) in all other mud samples, including S2, S3, S4 and S5. Yield point property was increased gradually in all samples based on the amount of the NCs added, except, the change happened from S1 to S2 which was higher than the changes obtained for the other samples because no NCs exist in S1 and this proves the effect of NCs on yield point. However, the values of both initial and final gel strength were raised steadily from S1 to S4 and increased sharply in S5 and S6 due to the higher concentrations of NCs. For instance, the measured values of initial gel strength and final gel strength for S5 were 29 and 35 lb/100 ft^2, respectively. In S6 they were improved by 40% when the concentration of NCs was increased from 0.2 to 0.5 wt.%.

Furthermore, from Fig. 8, for all samples of drilling fluids with and without NCs, it is shown that the viscosity is inversely related to shear rates. For S6 with the highest concentration of NCs, the best thinning behaviour with a viscosity of 174 cP at 5.1 s^{-1} shear rate was achieved. However, the WB drilling fluid without NCs has the worst thinning behaviour and rheological performance with 13 cP viscosity at a 5.1 s^{-1} shear rate. Fig. 10 shows the shear stress–shear rate relationship for the prepared drilling mud samples. For all samples, the shear rates increased on increasing the shear stresses, but the increments for the nanofluid samples S5 and S6 were higher compared to what was gained in other drilling fluids. Thus, the viscosity slope gradient of the shear stresses–shear rates plot was also higher for these two drilling nanofluids.

3.4 Filtration properties

The fluid loss and the thickness of the mud cake were measured for all nanofluid-modified drilling mud samples and compared to the base drilling mud at different concentrations of NCs (see Table 3). S1, the base drilling mud, shows a fluid loss of about 10.8 ml, while it was reduced in S2, S3, S4, S5 and S6 by 5.6, 18.5, 36, 44.4 and 53.7% to 10.2, 8.8, 8, 6 and 5 ml, respectively. Meanwhile, the effect of the NCs on the filter cake was more significant compared to its effect on the fluid loss reduction. The 4 mm mud cake thickness for the WB was reduced by 92.5% when NCs at different concentrations were added. The lowest thickness and minimum fluid loss was obtained with S6 by adding 0.5 wt.% NCs into WB. This sample contained the highest concentration of added NCs.

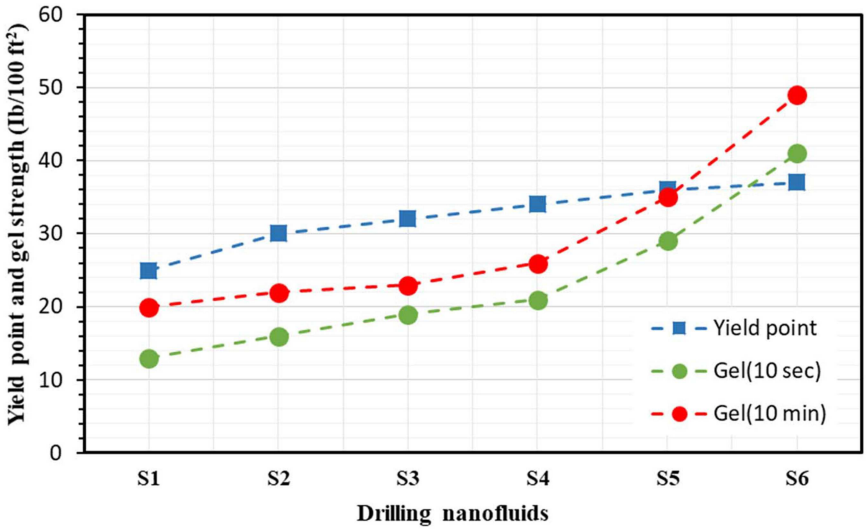

Fig. 9 *Yield point and gel strength properties of different samples of drilling muds with different concentrations of SiO_2@ZnO@Xanthan NC*

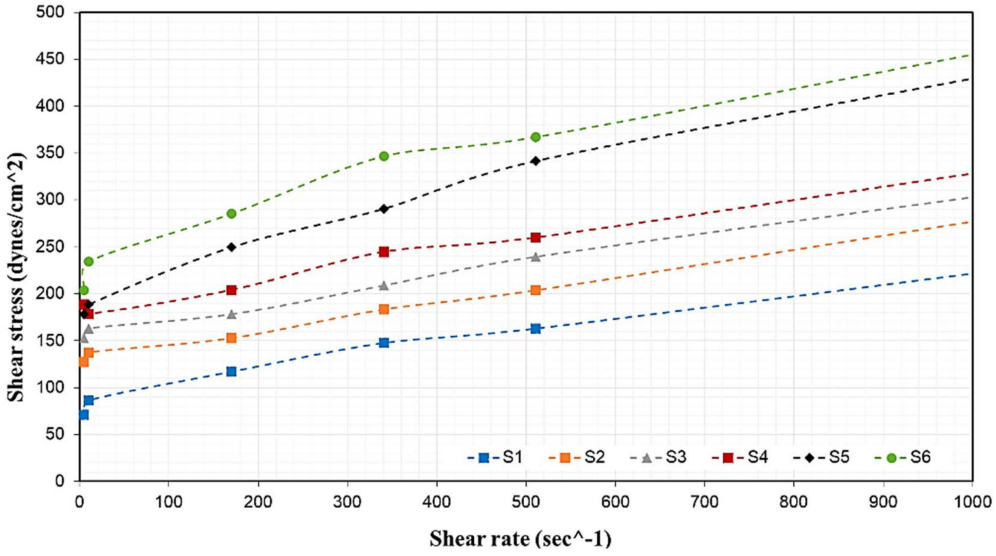

Fig. 10 *Shear stress–shear rate plot for the fluids with different concentrations SiO_2@ZnO@Xanthan NCs showing the positive co-variation of the two values*

Table 3 Filtration properties of the NC base drilling fluid

Filtration properties	Drilling mud sample					
	S1 (base mud)	S2	S3	S4	S5	S6
fluid loss, ml	10.8	10.2	8.8	8	6	5
% decrease over BS	—	5.6	18.5	26	44.4	53.7
filter cake, mm	4	3.5	3	2	0.5	0.3
% decrease over BS	—	12.5	25	50	87.5	92.5

Hence, it can be strongly suggested that the concentration of NCs within the nanofluid samples had a significant effect on filtration properties.

Furthermore, Fig. 11 illustrates the fluid loss and filter cake characteristics of different samples (S2, S3, S4, S5 and S6) of prepared drilling nanofluid with the base sample of the drilling fluid (S1). From Fig. 11, it can be seen that the volume of the fluid loss and the thickness of the mud cake were decreased on increasing the percentage of NCs within the drilling mud. This improvement in filtration properties of the drilling fluid is caused by the effect of silicon dioxide and zinc oxide NPs existing within the NCs because of providing a high surface area. In terms of fluid loss, a smooth change or reduction is obtained ranging from S1 to S6 for the same period of time (Fig. 11*a*). Whereas, a sharp reduction in the thickness of the mud cake was obtained in S5, when the concentration of NCs within the drilling nanofluid increased from 0.1 to 0.2 wt.%. Thus, the minimum thicknesses of the mud cake were found in S5 and S6 nanofluids with the concentrations of 0.2 and 0.5 wt.% of NCs, respectively (Fig. 11*b*).

In spite of illustrating the effect of NCs on filtration properties above, the distribution of the NCs including SiO_2 and ZnO NPs on the mud cake was also identified using SEM morphology with the scale of 5 µm as shown in Fig. 12. From the figure, which is for the mud cake obtained from the S2 nanofluid, it is obvious that some NPs with sizes <100 nm were visible on the surface of the mud cake, even penetrated into the deep. The presence of these nano-sized materials on the surface or in the depth of the mud cake is a good indication of approving the effect of NCs on filtration properties in terms of reducing the thickness of the mud cake and minimising the fluid loss into permeable formation. From measuring the chemical composition of the identified NCs on the

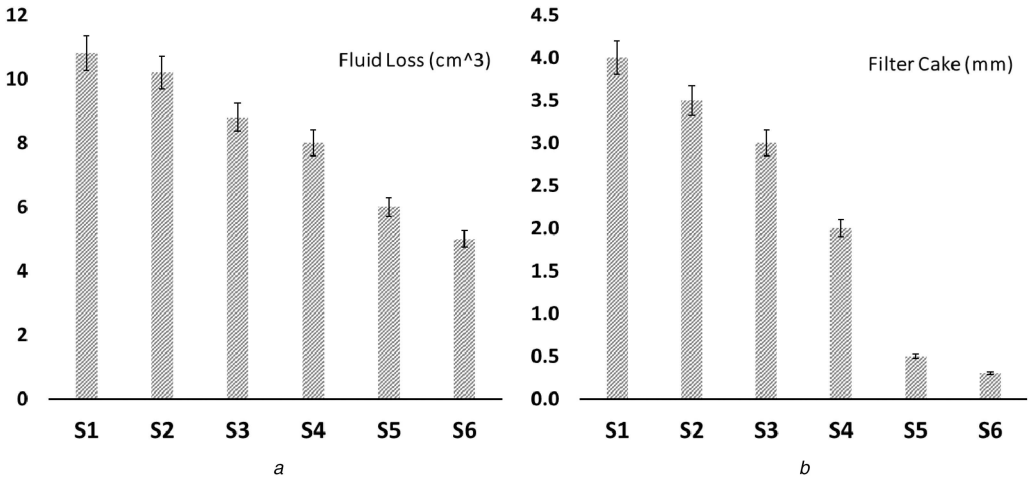

Fig. 11 *Filtration properties of six drilling fluid samples with and without the presence of NCs*
(a) Fluid loss volumes of muds measured in a cylinder from the outlet of the filter press, ***(b)*** Filter cake thicknesses of used muds measured on the filter paper

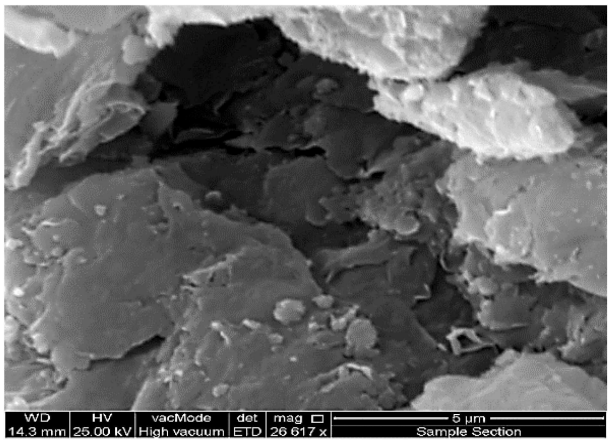

Fig. 12 *SEM micrograph of the mud filter cake with a NC of S5 mud (0.2 wt.% of NCs)*

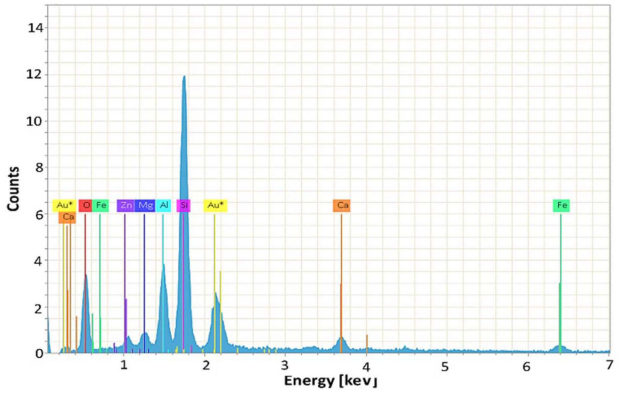

Fig. 13 *EDX spectrum of the NCs on the mud cake of S5 mud (0.2 wt.% of NCs)*

mud cake using EDX, some elements were witnessed, such as gold (Au), calcium (Ca), oxygen (O), iron (Fe), zinc (Zn), magnesium (Mg) and silicon (Si) as shown in Fig. 13. The presence of the gold was due to the coating of the sample by this element. Silicon and zinc were present as NPs within the SiO_2@ZnO@Xanthan NCs and their identification on the mud cake by EDX was a good indication of their role. The EDX analysis shows that the amount of the silica dioxide is the highest compared with the other elements reaching about 16% of the bulk composition.

4 Conclusion

In this work, a novel nano-water based drilling fluid was prepared by adding green synthesised SiO_2@ZnO@Xanthan NC as an additive to the base drilling fluid. The SiO_2@ZnO@Xanthan NC was synthesised and developed from pomegranate seed extract in a green and economical way without using any harsh conditions and hazardous reagents and materials. The production of these NCs was confirmed by conducting the characterisation analysis using UV-Vis, XRD, FE-SEM and EDS techniques. From studying the rheological and filtration properties of the nano-drilling fluid, it was identified that the plastic viscosity, yield point, gel strength and thinning behaviour of mud were increased by increasing the concentration of NCs. Besides the effect of the large surface of NCs, the improvement of these properties strongly returned to the presence of bioactive phytochemicals on the nanosurface. In addition, the thickness of the mud cake and fluid loss were reduced by about 92% compared to the WB.

5 References

[1] Samuel, G.R., Azar, J.J., Aideyan, P., *et al.*: 'Applied drilling engineering optimization', 2017

[2] Song, K., Wu, Q., Li, M., *et al.*: 'Water-based bentonite drilling fluids modified by novel biopolymer for minimizing fluid loss and formation damage', *Colloids Surf. A, Physicochem. Eng. Aspects*, 2016, **507**, pp. 58–66

[3] Abdo, J., Haneef, M. D.: 'Clay nanoparticles modified drilling fluids for drilling of deep hydrocarbon wells', *Appl. Clay Sci.*, 2013, **86**, pp. 76–82

[4] Baba Hamed, S., Belhadri, M.: 'Rheological properties of biopolymers drilling fluids', *J. Petrol. Sci. Eng.*, 2009, **67**, (3), pp. 84–90

[5] Moon, R. J., Martini, A., Nairn, J., *et al.*: 'Cheminform abstract: cellulose nanomaterials review: structure, properties and nanocomposites', *ChemInform*, 2011, **42**, (42), pp. 3941–3994

[6] Li, M.-C., Wu, Q., Song, K., *et al.*: 'Cellulose nanoparticles: structure–morphology–rheology relationships', *ACS Sustain. Chem. Eng.*, 2015, **3**, (5), pp. 821–832

[7] William, J. K., Ponmani, S., Samuel, R., *et al.*: 'Effect of CuO and ZnO nanofluids in xanthan gum on thermal, electrical and high pressure rheology of water-based drilling fluids', *J. Petrol. Sci. Eng.*, 2014, **117**, pp. 15–27

[8] Sadeghalvaad, M., Sabbaghi, S.: 'The effect of the TiO_2/polyacrylamide nanocomposite on water-based drilling fluid properties', *Powder Technol.*., 2015, **272**, pp. 113–119
[9] Nasser, J., Jesil, A., Mohiuddin, T.*, et al.*: 'Experimental investigation of drilling fluid performance as nanoparticles', *World J. Nano Sci. Eng.*, 2013, **3**, (3), pp. 57–61
[10] Al-Zubaidi, N. S., Alwasiti, A.A., Mahmood, D.*, et al.*: 'A comparison of nano bentonite and some nano chemical additives to improve drilling fluid using local clay and commercial bentonites', *Egypt. J. Petrol.*, 2017, **26**, (3), pp. 811–818
[11] Barry, M.M., Jung, Y., Lee, J.-K.*, et al.*: 'Fluid filtration and rheological properties of nanoparticle additive and intercalated clay hybrid bentonite drilling fluids', *J. Petrol. Sci. Eng.*, 2015, **127**, pp. 338–346
[12] Schmid, G.: 'Large clusters and colloids. Metals in the embryonic state', *Chem. Rev.*, 1992, **92**, (8), pp. 1709–1727
[13] Li, F., Zhang, B., Dong, S.*, et al.*: 'A novel method of electrodepositing highly dispersed nano palladium particles on glassy carbon electrode', *Electrochim. Acta*, 1997, **42**, (16), pp. 2563–2568
[14] Ranjbar, M., Taher, M. A., Sam, A.: 'Facile single-step synthesis of SiO_2-coated ZnO nanorod as hydrophobic layer by hydrothermal method', *J. Cluster Sci.*, 2015, **27**, (1), pp. 105–114
[15] Ranjbar, M., Taher, M. A., Sam, A.: 'Single-step synthesis of SiO_2–TiO_2 hydrophobic core–shell nanocomposite by hydrothermal method', *J. Cluster Sci.*, 2015, **27**, (2), pp. 583–592
[16] Kim, S., Park, J., Jang, Y.*, et al.*: 'Synthesis of monodisperse palladium nanoparticles', *Nano Lett.*, 2003, **3**, (9), pp. 1289–1291
[17] Nemamcha, A., Rehspringer, J.-L., Khatmi, D.*, et al.*: 'Synthesis of palladium nanoparticles by sonochemical reduction of palladium(II) nitrate in aqueous solution', *J. Phys. Chem. B*, 2006, **110**, (1), pp. 383–387
[18] Wei, Z., Xu, C., Li, B.*, et al.*: 'Application of waste eggshell as low-cost solid catalyst for biodiesel production', *Bioresour. Technol.*, 2009, **100**, (11), pp. 2883–2885
[19] Xuan, S., Wang, Y.-X.J., Yu, J.C.*, et al.*: 'Preparation, characterization, and catalytic activity of core/shell Fe_3O_4@Polyaniline@Au nanocomposites', *Langmuir*, 2009, **25**, (19), pp. 11835–11843
[20] Issaabadi, Z., Nasrollahzadeh, M., Sajadi, S.M.*, et al.*: 'Green synthesis of the copper nanoparticles supported on bentonite and investigation of its catalytic activity', *J. Cleaner Prod.*, 2017, **142**, pp. 3584–3591
[21] Nasrollahzadeh, M., Atarod, M., Sajadi, S.M.*, et al.*: 'Biosynthesis, characterization and catalytic activity of Cu/RGO/Fe_3O_4 for direct cyanation of aldehydes with $K_4[Fe(CN)_6]$', *J. Colloid Interface Sci.*, 2017, **486**, pp. 153–162
[22] Ali, J. A., Kolo, K., Manshad, A.K.*, et al.*: 'Modification of LoSal water performance in reducing interfacial tension using green ZnO/SiO_2 nanocomposite coated by xanthan', *Appl. Nanosci.*, 2019, **9**, pp. 397–409. doi:10.1007/s13204-018-0923-5
[23] Sajadi, S. M., Kolo, K., Pirouei, M.*, et al.*: 'Natural iron ore as a novel substrate for the biosynthesis of bioactive-stable ZnO@CuO@iron ore NCs: a magnetically recyclable and reusable superior nanocatalyst for the degradation of organic dyes, reduction of Cr(vi) and adsorption of crude oil aromatic compounds, including PAHs', *RSC Adv.*, 2018, **8**, (62), pp. 35557–35570
[24] Ali, J. A., Kolo, K., Khaksar Manshad, A.*, et al.*: 'Low-salinity polymeric nanofluid-enhanced oil recovery using green polymer-coated ZnO/SiO_2 nanocomposites in the upper Qamchuqa formation in Kurdistan Region, Iraq', *Energy Fuels*, 2019, **33**, (2), pp. 927–937. doi:10.1021/acs.energyfuels.8b03847
[25] Ali, J., Sajadi, S., Kolo, K.*, et al.*: 'Green synthesis of ZnO/SiO_2 nanocomposite from pomegranate seed extract: coating by natural xanthan polymer and its characterizations', *Micro Nano Lett.*, 2019, **14**, pp. 638–641. doi:10.1049/mnl.2018.5617